

Recombinant Gas6 augments Axl and facilitates immune restoration in an intracerebral hemorrhage mouse model

Lu-sha Tong^{1,2,*}, An-wen Shao^{1,3,*}, Yi-bo Ou^{1,4}, Zhen-ni Guo^{1,5}, Anatol Manaenko¹, Brandon J Dixon¹, Jiping Tang², Min Lou² and John H Zhang¹

Abstract

Axl, a tyrosine kinase receptor, was recently identified as an essential component regulating innate immune response. Suppressor of cytokine signaling 1 and suppressor of cytokine signaling 3 are potent Axl-inducible negative inflammatory regulators. This study investigated the role of Axl signaling pathway in immune restoration in an autologous blood-injection mouse model of intracerebral hemorrhage. Recombinant growth arrest-specific 6 (Gas6) and R428 were administered as specific agonist and antagonist. In vivo knockdown of Axl or suppressor of cytokine signaling 1 and suppressor of cytokine signaling 3 by siRNA was applied. After intracerebral hemorrhage, the expression of endogenous Axl, soluble Axl, and Gas6 was increased, whereas the expression of suppressor of cytokine signaling 1 and suppressor of cytokine signaling 3 was inhibited. Recombinant growth arrest-specific 6 administration alleviated brain edema and improved neurobehavioral performances. Moreover, enhanced Axl phosphorylation with cleavage of soluble Axl (sAxl), and an upregulation of suppressor of cytokine signaling 1 and suppressor of cytokine signaling 3 were observed. In vivo knockdown of Axl and R428 administration both abolished the effect of recombinant growth arrest-specific 6 on brain edema and also decreased the expression suppressor of cytokine signaling 1 and suppressor of cytokine signaling 3. In vivo knockdown of suppressor of cytokine signaling 1 and suppressor of cytokine signaling 3 aggravated cytokine releasing despite of recombinant growth arrest-specific 6. In conclusion, Axl plays essential role in immune restoration after intracerebral hemorrhage. And recombinant growth arrest-specific 6 attenuated brain injury after intracerebral hemorrhage, probably by enhancing Axl phosphorylation and production of suppressor of cytokine signaling 1 and suppressor of cytokine signaling 3.

Keywords

Axl, Gas6, suppressor of cytokine signaling 1, suppressor of cytokine signaling 3, intracerebral hemorrhage

Received 15 April 2016; Revised 6 June 2016; Accepted 7 June 2016

Introduction

Spontaneous intracerebral hemorrhage (ICH) remains a devastating disease causing high mortality and morbidity.¹ Accumulating evidence has demonstrated that neurological deficiencies in ICH are largely attributed to excessive activation of the innate immune response.^{2–5} Recently, intrinsic negative regulation following the engagement of innate immune response was highlighted.⁶ Yet, the auto-regulatory mechanism involved in ICH remains to be elucidated.

Axl, a member of TAM (Tyro3, Axl and Mer) receptor tyrosine kinases, has recently been underscored as one critical regulator for innate immune response.^{6,7}

¹Department of Anesthesiology, School of Medicine, Loma Linda University, CA, USA

²Department of Neurology, School of Medicine, the 2nd Affiliated Hospital of Zhejiang University, Hangzhou, China

³Department of Neurosurgery, School of Medicine, the 2nd Affiliated Hospital of Zhejiang University, Hangzhou, China

⁴Department of Neurosurgery, Tong-ji Hospital, Wuhan, China

⁵Department of Neurology, Neuroscience Center, The First Hospital of Jilin University, Changchun, China

*These authors contribute equally to this work.

Corresponding authors:

John H Zhang, Department of Anesthesiology, Loma Linda University, 11041 Campus St, Risley Hall, Loma Linda, CA 92354, USA.

Email: johnzhang3910@yahoo.com

Min Lou, Department of Neurology, The 2nd Affiliated Hospital of Zhejiang University, School of Medicine, Hangzhou, China, 310009.

Email: loumingxc@vip.sina.com

Studies in peripheral myeloid cells demonstrated that Axl can be activated by its ligand growth arrest-specific 6 (Gas6), and the downstream signaling of Axl may include the suppressor of cytokine signaling 1, 3 (SOCS1, SOCS3).^{8,9} In addition, administration of exogenous Gas6 can attenuate inflammatory injury in autoimmune deficiencies in mice. Van den Brand et al.¹⁰ found that localized injection of adenovirus overexpressing Gas6 alleviated arthritis inflammation. Gruber et al.¹¹ also reported inflammatory inhibition by intraventricular delivery of Gas6 during experimental autoimmune encephalomyelitis (EAE). However, no study addressed whether or how Axl is involved in ICH, especially in regulating innate immune response after ICH.

Thus, in the present study, we tended to characterize the role and mechanisms of the Axl signaling pathway in an autologous blood-injection ICH mouse model. We hypothesized that Axl may be triggered by innate immune response after ICH and played a key role in immune restoration. SOCSs protein may be enrolled in this self-protective response to inhibit cytokine releasing, whereas administration of Axl exogenous ligand (rGas6) may augment Axl activation, facilitate negative regulatory effect of SOCSs, and help immune restoration after ICH.

Materials and methods

This report is conducted according to the ARRIVE guidelines

Animals

All animal protocols and procedures for this study were approved by the Institutional Animal Care and Use Committee at Loma Linda University. The study followed the Guide for The care and the Use of Laboratory Animals (National Research Council) and complied with the ARRIVE guidelines for reporting in vivo experiments. Two-hundred and twelve eight-week-old male CD1 mice (weight=22–25 g; Charles River, Wilmington, MA) were subjected to this study. Six mice included died of severe neurological deficiency, and three more mice were excluded because of anesthesia complication (see Supplementary Information 1, SI Table 1). All mice were housed in filter-top cages and fed a standard diet, with a 12-h light/dark cycle. Free access to food and water as well as controlled temperature and humidity were provided.

Autologous blood-injection ICH model

A stereotactically guided, autologous whole blood double injection model was used to mimic right-sided

intrastratial bleeding as previously published.^{12,13} Briefly, mice were anesthetized with ketamine (100 mg/kg) and xylazine (10 mg/kg) (2:1, intraperitoneal injection) and fixed prone in a stereotactic frame (Kopf Instruments, Tujunga, CA); 30 μ L autologous arterial blood without anticoagulation was obtained from the central artery of the tail and injected into the basal ganglion (0.2 mm anterior, 2.0 mm lateral to the bregma, and 3.5 mm deep). The syringe was fixed onto the microinjection pump, while the needle was stereotactically inserted into the brain through the burr hole. At first the needle was stopped at 0.5 mm above the target position and 5 μ L of blood was delivered at a rate of 2 μ L/min. The remaining 25 μ L blood was injected 5 min later than the first bolus at 3.5 mm depth at a rate of 2 μ L/min. The needle was held in place for 10 min more after injection and withdrawn slowly to allow the blood coagulation. Bone wax was then applied to seal the craniotomy, and the scalp was closed with suture. Mice in the sham group were subjected to sterile saline injection only.

Experimental design

Six separate experiments were conducted (see Supplementary Information 2, SI Figure 1).

Experiment I. To determine the time course of endogenous Gas6, Axl, and soluble Axl (sAxl) after ICH, Western blots analysis for their expression were performed using the peri-hematoma tissue in the ipsilateral/right hemisphere of each group at 3, 6, 12, 24, and 72 h after ICH insult. Sham group received saline injection of the same volume (n=6 each time point).

Experiment II. Double immunofluorescent staining was applied to characterize the Axl localization with neuronal specific nuclear protein (NeuN), glial fibrillary acidic protein (GFAP), and ionized calcium-binding adaptor molecule 1 (Iba-1) in sham and ICH groups at 24 h, respectively (n=3 each group).

Experiment III. To assess the effect of intranasal administration of exogenous recombinant Gas6 1 h after ICH, brain water content and neurobehavioral functions were performed at 24 and 72 h after surgery. The mice were divided into four groups: sham, ICH+vehicle (PBS), ICH+rGas6 (0.1 mg/kg), and ICH+rGas6 (0.4 mg/kg) (n = 6/8).

Experiment IV. Immunoprecipitation at 24 h was applied to detect the phosphorylated Axl and soluble Axl in sham, ICH with vehicle and ICH with recombinant growth arrest-specific 6 (rGas6) treatment groups (n=6 each group). The time course of Gas6, Axl,

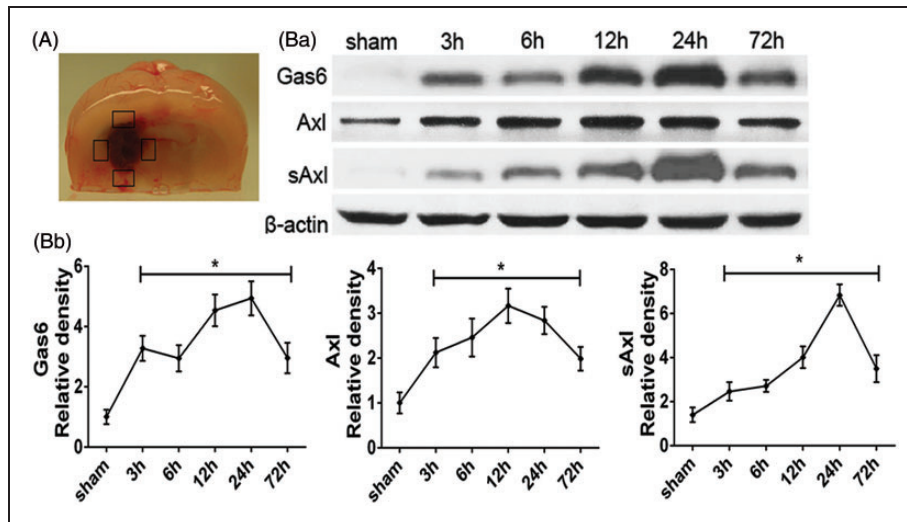


Figure 1. Expression profiles of endogenous Gas6, Axl and soluble Axl after ICH in mice. (a) Peri-hematoma tissue was obtained for Western blot. (Ba) Western blot assay showing endogenous expression profiles and (Bb) quantification results of Gas6, Axl and soluble Axl in sham and ICH model for 3, 6, 12, 24, and 72 h. Error bars represented mean \pm standard deviation. * $p < 0.05$ versus sham.

soluble Axl (sAxl) with treatment of recombinant Gas6 was evaluated by Western blots as well. The expression of SOCS1 and SOCS3 with rGas6 treatment was also evaluated by Western blots through a time course of 72 h after ICH or sham surgery. The samples for sham and ICH groups were shared from Experiment I.

Experiment V. R428, a specific antagonist for Axl, was formulated with 1% dimethyl sulfoxide and sterilized saline to a final concentration of 0.5 mg/mL. Intraperitoneal administration of R428 was performed to further clarify the essential role of Axl signaling pathway in the context of ICH. Three groups were divided: sham, ICH+vehicle (saline), and ICH+R428 (100 mg/kg). Brain water content and modified Garcia score were evaluated at 24 h ($n=6/8$ each group). Western blot was performed to evaluate the cytokine releasing of interleukin (IL)-1 β and tumor necrotic factor (TNF)- α . The ICH group samples applied in Western blot assay were shared with Experiment I and the neurological score data of sham group were share from Experiment III.

Experiment VI. In vivo knockdown of Axl or the SOCS1, 3 was performed by intracerebroventricular injection of siRNA 48 h before ICH surgery and then followed with rGas6 (0.4 mg/kg) treatment. The sham, vehicle, and rGas6 groups shared neurobehavioral data from Experiment III. Modified Garcia score was evaluated at 24 h after ICH insult and Western blots assay were applied to detect the expression of SOCS1, SOCS3, IL-1 β , and TNF- α ($n=6$). The Western blot and immunoprecipitation samples were shared with Experiments I and IV, and the neurobehavioral data were shared with Experiment III.

Intranasal administration of rGas6

Intranasal administration was performed as previously described.¹⁴ PBS or rGas6 (0.1 mg/kg or 0.4 mg/kg) dissolved in PBS was administrated. A total volume of 20 μ L was delivered into the bilateral nares, alternating one naris at a time; 12 μ g rGas6 was given to all the experimental groups, except for those using the low dose of 0.1 mg/kg.

Neurobehavioral function assessment

Neurobehavioral functions were assessed by modified Garcia neurological score, forelimb placing test, and corner turn at 24 and 72 h after surgery, as previously reported.^{15,16} Seven items were included in modified Garcia score: spontaneous activity; body proprioception; sense of vibrissae touch; limb symmetry; forepaw outstretching; and response to whisker stimulation; and climbing. The evaluation consisted of seven tests that can be scored from either 0–3 (spontaneous activity, limb symmetry, sense of vibrissae touch, and forepaw outstretching) or 1–3 (climbing, body proprioception, and response to whisker stimulation). In the corner turn test, animals were allowed to enter into a corner with a 30 $^{\circ}$ C angle. The animals will try to exit the corner with either a right turn or left turn. Ten trials were performed for each animal, and the percentage of right turns in 10 trials was calculated. Forelimb placing test was conducted when the animal was held by their torsos, which allowed the forelimb to hang free. When the animals were approaching the corner edge of a countertop, the forelimb placing ipsilateral to the stimulated vibrissae was recorded.

The percentage of appropriate forelimb placing in 10 trials was calculated. Two experienced investigators blinded to animal groups performed these tests and the mean value was defined as the final score for each mouse.

Brain water content measurement

Brain water content was measured as previously reported.¹⁷ Briefly, mice were decapitated under deep anesthesia. Next, brains were immediately removed, and the surface water on the cerebral tissues was blotted with filter paper. The brains were then divided into five parts (ipsilateral and contralateral cortex, ipsilateral and contralateral basal ganglia, and cerebellum). Each part was weighed on an electric analytic balance to obtain the wet weight and then dried at 100°C for 24 h to obtain the dry weight. Brain water content was calculated using the following formula: brain water content (%) = (wet weight - dry weight) / wet weight × 100%.

In Vivo RNAi

In vivo RNAi was performed as previously described.¹⁸ For Axl in vivo RNAi, Accell SMART pool siRNA duplexed of three different siRNA were applied by intraventricular injection as previously described. Mouse Axl-siRNA, SOCS1-siRNA and SOCS3-siRNA (0.5 nmol/2 µL, Dharmacon, Lafayette, CO), and negative control siRNA (0.5 nmol/2 µL, Dharmacon, Lafayette, CO) were delivered into the ipsilateral ventricle (1.0 mm lateral of the bregma, 3.2 mm deep) according to the manufacturer's instructions, at a rate of 0.5 µL/min.

Western blots

Western blots was performed as previously described.¹⁹ Primary antibodies used were goat polyclonal anti-Axl (Santa Cruz Biotechnology, Santa Cruz, CA, used for total Axl), mouse monoclonal anti-Gas6 (R&D system, Minneapolis, MN), mouse monoclonal anti-Axl (R&D system, , used for soluble Axl), mouse monoclonal anti-SOCS1 (R&D system), mouse monoclonal anti-SOCS3 (R&D system), goat polyclonal anti-IL-1β (Abcam, Cambridge, MA), and goat polyclonal anti-tumor necrotic factor (TNF)-α (Abcam, Cambridge, MA). Goat polyclonal β-actin and the secondary antibodies were all from Santa Cruz Biotechnology. ECL Plus chemiluminescence reagent kit (Amersham Biosciences, Arlington Heights, IL) was used to probe immunoblots.

Immunoprecipitation assay

The procedure of immunoprecipitation was carried out following the manufacturer's guidelines as previously

described.⁸ Protein extracts were precipitated by goat polyclonal anti-Axl (Santa Cruz Biotechnology, Santa Cruz, CA, used for total Axl) and protein A/G PLUS-Agarose (Santa Cruz Biotechnology, Santa Cruz, CA). After washing and centrifuging, the pellet was collected and re-suspended and boiled with loading buffer. Goat polyclonal anti-Axl (Santa Cruz Biotechnology, Santa Cruz, CA, used for total Axl), mouse monoclonal anti-Axl (R&D system, used for soluble Axl), and anti-phosphorylated tyrosine (Millipore, Billerica, MA) were applied to probe Axl, soluble Axl, and phosphorylated Axl by Western blots. IgG (Santa Cruz Biotechnology, Santa Cruz, CA) worked as an internal loading control.

Immunofluorescence staining

Immunofluorescence staining was performed as previously described.¹⁸ Coronal frozen slices (10 µm) were obtained with cryostat (Leica CM3050S-3-1-1, Bannockburn, IL) and permeabilized with 0.3% Triton X-100 in PBS for 30 min. Sections were blocked with 5% donkey serum for 1 h and incubated at 4°C overnight with primary antibodies: goat polyclonal anti-Axl (Santa Cruz Biotechnology, Santa Cruz, CA, used for total Axl), mouse monoclonal anti-Axl (R&D system, used for soluble Axl), rabbit polyclonal anti-NeuN (Abcam, Cambridge, MA), rabbit polyclonal anti-Iba-1 (Abcam, Cambridge, MA), and rabbit polyclonal anti-GFAP (Abcam, Cambridge, MA) followed by incubation with appropriate fluorescence-conjugated secondary antibodies (Jackson ImmunoResearch, West Grove, PA) for 2 h at room temperature. The slices were visualized under a fluorescence microscope (Olympus BX51, Olympus Optical Co. Ltd, Japan), and pictures were taken with software MagnaFire SP 2.1B (Olympus, Melville, NY).

Statistics

All data were expressed as mean ± SD. Analysis was performed using SPSS version 22.0 (SPSS Inc.). Mean values were compared using Student *t* test for comparison between two groups. ANOVA or Kruskal-Wallis one-way analysis followed by post hoc Bonferroni test were used for multiple-group comparisons. Statistical significance was defined as *p* < 0.05.

Results

Endogenous Gas6, Axl and soluble Axl were upregulated after ICH

As demonstrated in Figure 1, endogenous expression of Gas6, Axl and soluble Axl was increased at 3 h after ICH and remained at high level at 72 h (Figure 1(Ba) and 1(Bb)). Gas6 and soluble Axl reached the highest

level at 24 h, whereas Axl arrived at the climax around 12 to 24 h ($p < 0.05$).

Endogenous Axl was expressed intracellularly in both microglia cells and neurons

Double immunofluorescent staining of Axl with neuronal specific nuclear protein (NeuN), GFAP, and ionized calcium-binding adaptor molecule 1 (Iba-1) (Figure 2) demonstrated that sham samples were rarely Axl positive and mostly expressed on neurons (Figure 2(a)). In contrast, after ICH, Axl was mainly localized in neurons and microglia cells 24 h after ICH (Figure 2(b)).

Exogenous rGas6 treatment improved neurobehavioral performance and reduced brain edema after ICH

Low (0.1 mg/kg) and high dosage (0.4 mg/kg) of recombinant Gas6 (rGas6) was intranasally applied 1 h after ICH. When compared to sham group, ICH mice receiving vehicle exhibited significantly worse neurobehavioral scores, including modified Garcia test ($p < 0.01$, Figure 3(a)), corner turn ($p < 0.01$, Figure 3(b)) and forelimb placing ($p < 0.01$, Figure 3(c)) at 24 and 72 h, as well as increased brain edema in ipsilateral basal ganglion ($79.58 \pm 0.71\%$ vs. $82.90 \pm 0.31\%$, $p < 0.01$, Figure 3(d)). However, ICH mice receiving high dose of rGas6 (0.4 mg/kg) demonstrated improved neurobehavioral performances and significantly decreased brain edema at both 24 ($80.98 \pm 0.72\%$ vs. $82.90 \pm 0.31\%$, $p < 0.01$, Figure 3(d)) and 72 h ($80.56 \pm 0.53\%$ vs. $82.46 \pm 0.43\%$, $p < 0.01$, Figure 3(d)), when compared to the vehicle group. No significant differences of neurobehavioral score were observed between ICH mice with and without low dose of rGas6 at 24 h, thus only high dose of rGas6 was evaluated at 72 h.

Exogenous rGas6 potentiated Axl phosphorylation and mediated upregulation of SOCS1 and SOCS3

Immunoprecipitation was applied to detect total Axl, phosphorylated Axl, and soluble Axl (Figure 4(a)) at 24 h after ICH. We verified that high dose of rGas6 did not increase the total expression of Axl when compared to the vehicle (Figure 4(a)). However, the phosphorylated Axl was significantly increased in ICH mice receiving the high dose of rGas6. Interestingly, the expression of soluble Axl also showed significant increase when comparing the rGas6 group with the vehicle group, which was consistent with the change of phosphorylated Axl (Figure 4(a)). Moreover, the Western blots illustrated different expression patterns of soluble Axl, SOCS1, and SOCS3 with rGas6

treatment over a time course of 72 h after ICH. There was an earlier elevation of Axl when the rGas6 group was compared with the ICH group (Figure 4(b) and Figure 1(Ba) and (Bb)). The generation of soluble Axl showed an increase at 3 h after ICH with rGas6 administration and remained high for 24 h (Figure 4(b) and Figure 1(Ba) and (Bb)). Additionally, when compared with the suppressed expression in the absence of rGas6 treatment (Figure 4(c)), the expression of SOCS1 and SOCS3 was both remarkably elevated from 6 h with rGas6 treatment (Figure 4(d)).

R428 aggravated brain edema and inflammatory cytokine releasing

A specific Axl antagonist, R428, was applied by intraperitoneal injection. Brain water content detection revealed more severe brain edema in response to R428 when compared to the vehicle at ipsilateral basal ganglion ($83.51 \pm 0.46\%$ vs. $82.98 \pm 0.41\%$, $p < 0.05$, Figure 5(a)). Although significant difference of the modified Garcia score was absent ($p > 0.05$, Figure 5(b)), the mortality in R428 treatment group was much higher than vehicle group (25% vs. 0). We also observed the expression of IL-1 β and TNF- α by Western blot and found that both were substantially elevated when the R428 group was compared to the vehicle group ($p < 0.05$, Figure 5(c)). Thus, R428 aggravated brain edema and promoted inflammatory cytokine releasing.

In vivo knockdown of Axl and R428 abolished the effect of rGas6 on inhibiting ICH neuroinflammation

To further verify the specificity of Gas6 as the ligand to Axl, we administrated Axl antagonist R428 and Axl siRNA in addition with rGas6. The knockdown efficacy was demonstrated by immunoprecipitation comparing the Axl siRNA with the control siRNA administration (Figure 6(a)). Additionally, immunoprecipitation showed that, not only was total Axl significantly inhibited by Axl siRNA administration, but also was the expression of phosphorylated Axl and soluble Axl, compared with control siRNA administration ($p < 0.05$, Figure 6(a)). Modified Garcia evaluated at 24 h after ICH insult demonstrated that the effect of rGas6 was abolished when si-Axl, R428, or si (SOCS1+SOCS3) were additionally applied ($p < 0.05$, Figure 6(b)), whereas the control siRNA did not change the neurobehavioral function with rGas6 administration ($p > 0.05$, Figure 6(b)). Western blots assay revealed a significant increase of SOCS1 and SOCS3 in rGas6 treatment group when compared with vehicle group (Figure 6(c)). However, this effect

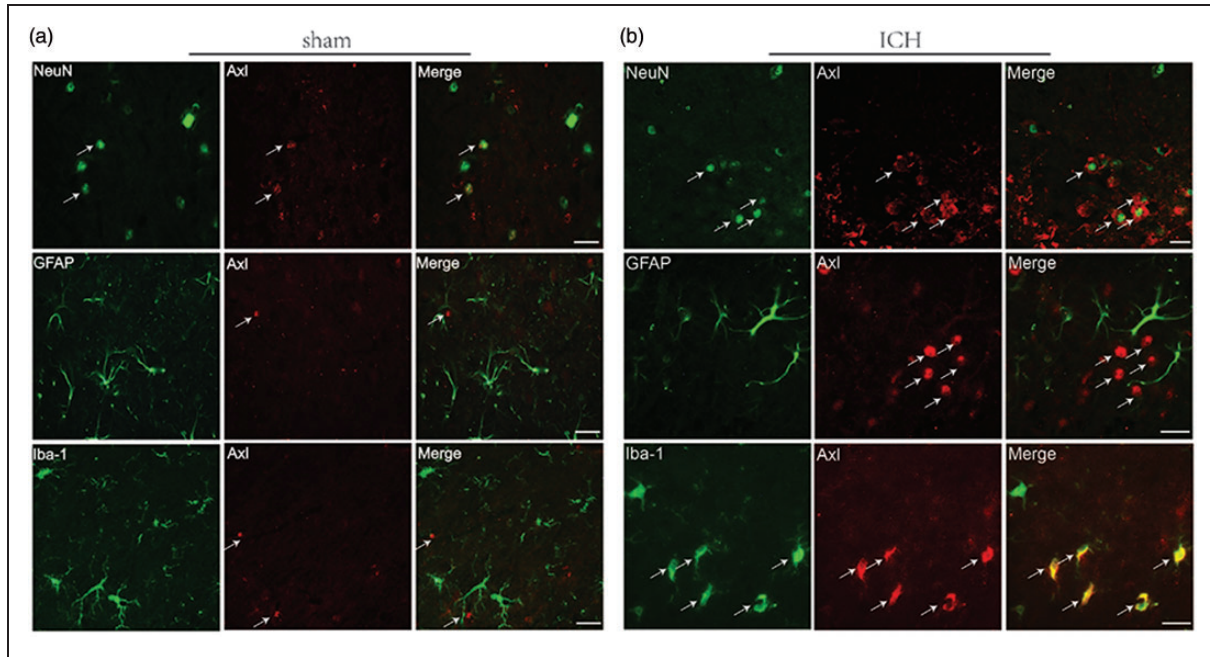


Figure 2. Endogenous Axl preferentially expressed on cellular membrane of neuron and microglia. Representative images of immunofluorescent staining to show the expression profile both in (a) sham and (b) ICH mice brain of Axl (red), respectively, with NeuN (green) marked neurons, GFAP (green) marked astrocytes and Iba-1 (green) marked microglia. Samples were obtained from peri-hematoma area 24 h following autologous blood-injection-induced ICH. Bar=20 μ m.

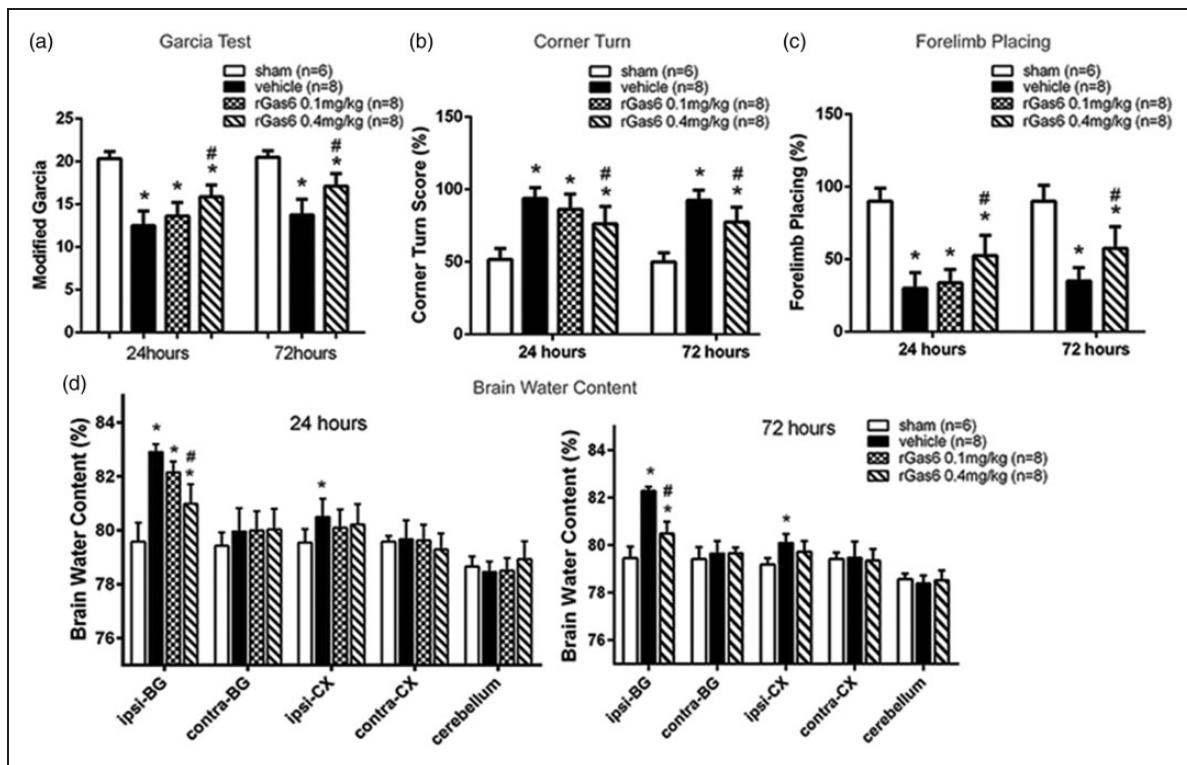


Figure 3. Exogenous recombinant Gas6 improved neurobehavioral performance and reduced the brain edema. (a) Modified Garcia test, (b) corner turn and (c) forelimb placing test at 24 and 72 h following operation in sham, vehicle, and rGas6 treatment groups (24 h: 0.1 mg/kg and 0.4 mg/kg; 72 h: 0.4 mg/kg). (d) Brain water content following operation in sham, vehicle, and rGas6 treatment groups (24 h: 0.1 mg/kg and 0.4 mg/kg; 72 h: 0.4 mg/kg). Brain sections were divided into five parts: ipsilateral basal ganglia (ipsi-BG), contralateral basal ganglia (contra-BG), ipsilateral cortex (ipsi-CX), contralateral cortex (contra-CX), and cerebellum. n=6/8 mice per group. Error bars represented median \pm standard deviation. * p < 0.05 versus sham; # p < 0.05 versus vehicle.

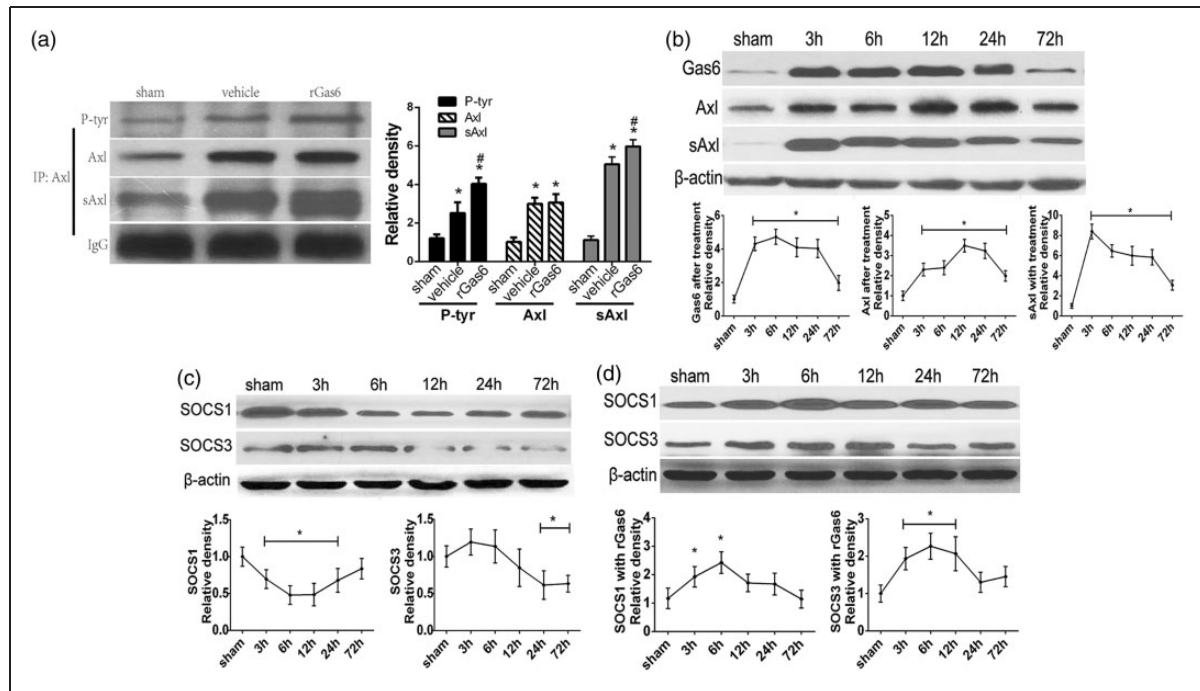


Figure 4. Exogenous rGas6 accelerated Axl phosphorylation and cleavage of soluble Axl, as well as changed the time course profile of SOCS1, SOCS3. (a) Immunoprecipitation assay showing Axl, phosphorylate-Axl and soluble Axl at 24 h following ICH or sham in mice. (b) Western blots showing expression of Gas6, Axl, and soluble Axl in sham and ICH mice in 72-h time course following ICH with rGas6 treatment. (c and d) Western blots showing the time course of SOCS1 and SOCS3 with (d) or without (c) rGas6. The sham group in (b, c and d) received PBS as a negative control. $n=6$ mice per group and per time point. $*p < 0.05$ versus vehicle for (a); $*p < 0.05$ versus Sham for (a), (b), (c), (d).

of SOCS1 and SOCS3 upregulation was abolished when R428 or si-Axl was added besides rGas6 (Figure 6(c)). Also, inflammatory cytokines such as IL-1 β and TNF- α were both suppressed by rGas6 treatment when compared to the vehicle group. Nevertheless, IL-1 β and TNF- α both showed rebound when rGas6 treatment was administrated at present with Axl-siRNA or R428 (Figure 6(c)).

In vivo knockdown of SOCS1 and SOCS3 abolished the inhibition effect of rGas6 on production of inflammatory cytokines

To investigate the anti-inflammatory role of SOCS1 and SOCS3, in vivo knockdown of these two negative regulator was processed. Western blots experiment showed that, SOCS1 and SOCS3 siRNA administration abolished rGas6-induced inhibition of IL-1 β and TNF- α when compared with rGas6 treatment group (Figure 6(c)). Also, the modified Garcia test showed worse outcomes when compared with the rGas6 treatment group ($p < 0.05$, Figure 6(b)). Furthermore, rebound of TNF- α and IL-1 β was observed compared to their expression in rGas6 treatment group, respectively (Figure 6(c)).

Discussion

Activation of the innate immune response contributes to the secondary injury and neurobehavioral deficits after ICH.^{2,13,20,21} Novel immune regulators have been targeted in pre-clinical research and clinical trials.^{22–24} Known as an innate immune regulator, Axl recently received widespread attention. It is proposed that Axl keeps silent in tolerogenic environments, whereas engaged as soon as inflammation occurs to damp inflammation and maintain immune homeostasis.^{7,25} In clinical practice, soluble Axl both in cerebral spinal fluid and plasma was found as a promising biomarker for intracranial aneurysm rupture.²⁶ However, little was known about Axl signal in the setting of ICH.

In present study, we firstly characterized the expression of this signaling pathway in an autologous blood-injection mice model through a time course. The upregulation of Gas6, Axl, and soluble Axl indicated that innate negative immune modulation was rapidly potentiated upon ICH insult. Along with our findings, other studies also showed Axl potentiated when triggered by inflammatory stimuli, such as toll-like receptors (TLRs) ligands,⁷ virus infections,²⁷ or in autoimmune diseases.²⁸

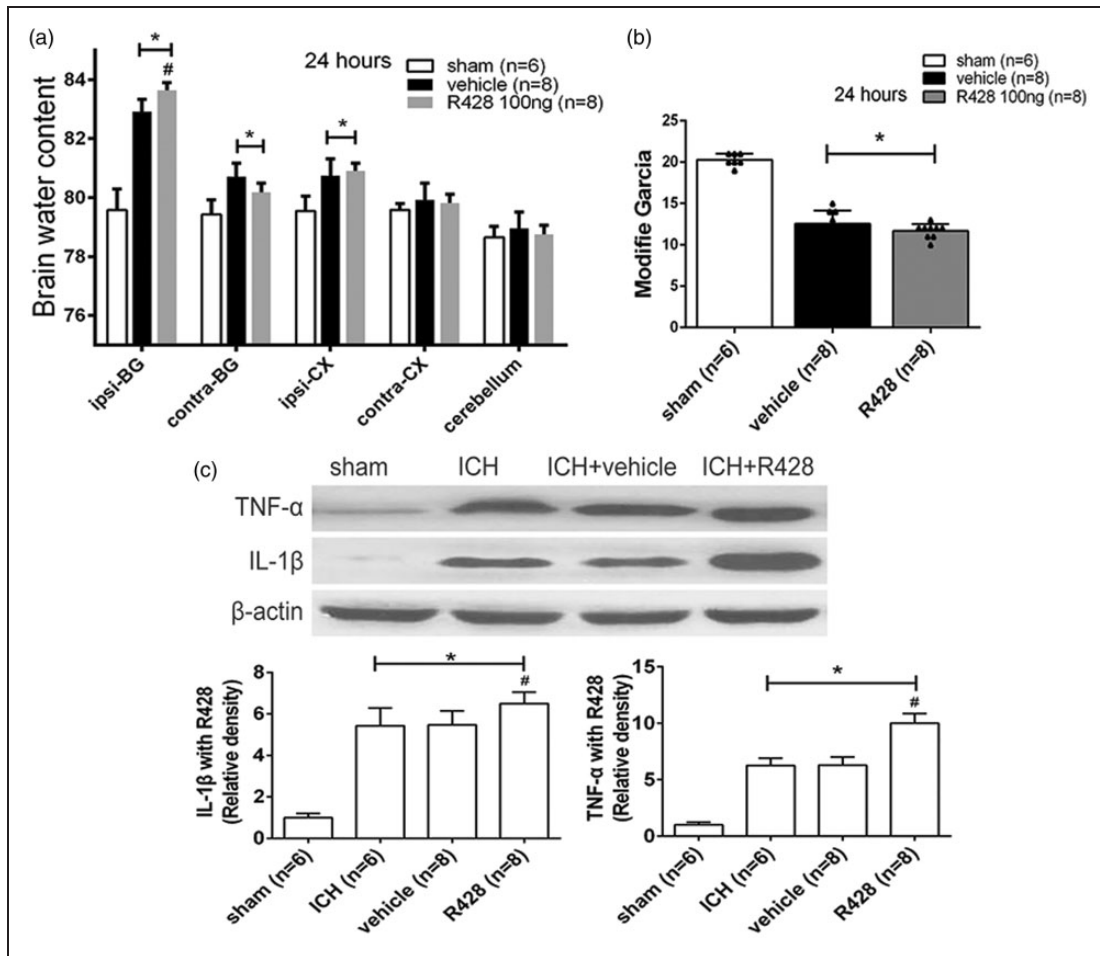


Figure 5. R428 worsened neurobehavioral deficits and aggravated cytokine releasing. (a) Brain water content following operation in sham, vehicle, and R428 treatment groups. Brain sections were divided into five parts: ipsilateral basal ganglia (ipsi-BG), contralateral basal ganglia (contra-BG), ipsilateral cortex (ipsi-CX), contralateral cortex (contra-CX), and cerebellum. (b) Showing modified Garcia test at 24 h following ICH in sham, vehicle and R428 groups. (c) Western blot assays for TNF- α and IL-1 β in sham, ICH, ICH+vehicle, ICH+R428 groups. $n=6/8$ mice per group. Error bars represented median \pm standard deviation. * $p < 0.05$ versus sham; # $p < 0.05$ versus vehicle for (a), (b), (c).

By applying exogenous rGas6, we observed neurobehavioral improvement as well as amelioration of brain edema. This finding was consistent with other studies using experimental autoimmune or inflammatory models.^{11,29} There were other studies suggesting that cleavage of a soluble form of Axl as an extracellular segment was resulted from Axl-Gas6 binding, and the intracellular phosphorylation of Axl was followed by further activation of downstream signals.^{30,31} Based on our findings, rGas6 only augmented the phosphorylation of Axl and cleavage of soluble Axl, rather than impeding the expression of total Axl. Thus, we may infer that rGas6 could only serve as a helper in inflammatory settings when total Axl expression was already potentiated. Additionally, our results also implicated that phosphorylation was required for Axl-dependent immune restoration, which was in accordance with the

generation of soluble Axl. Some oncological studies suggested soluble Axl as an antagonist for Gas6, by preventing Gas6 binding with the intracellular total Axl.³² We speculate that during ICH, the endogenous immune regulation is possibly limited by the generation of soluble Axl which blocks the continuous binding between Gas6 and total Axl. By applying exogenous rGas6, this barrier may be overcome and the Axl signaling pathway may be augmented.

From decades ago, SOCSs protein were recognized to suppress cytokines, such as IL-6, IL-4, and IL-1.³³⁻³⁵ In our study, expression of SOCS1 and SOCS3 was inhibited during the time course of 72 h, and reversed with exogenous rGas6-administration. In vivo knockdown of both SOCS1 and SOCS3 before rGas6-treatment showed aggravated cytokine releasing and unfavorable neurologic outcomes. These data

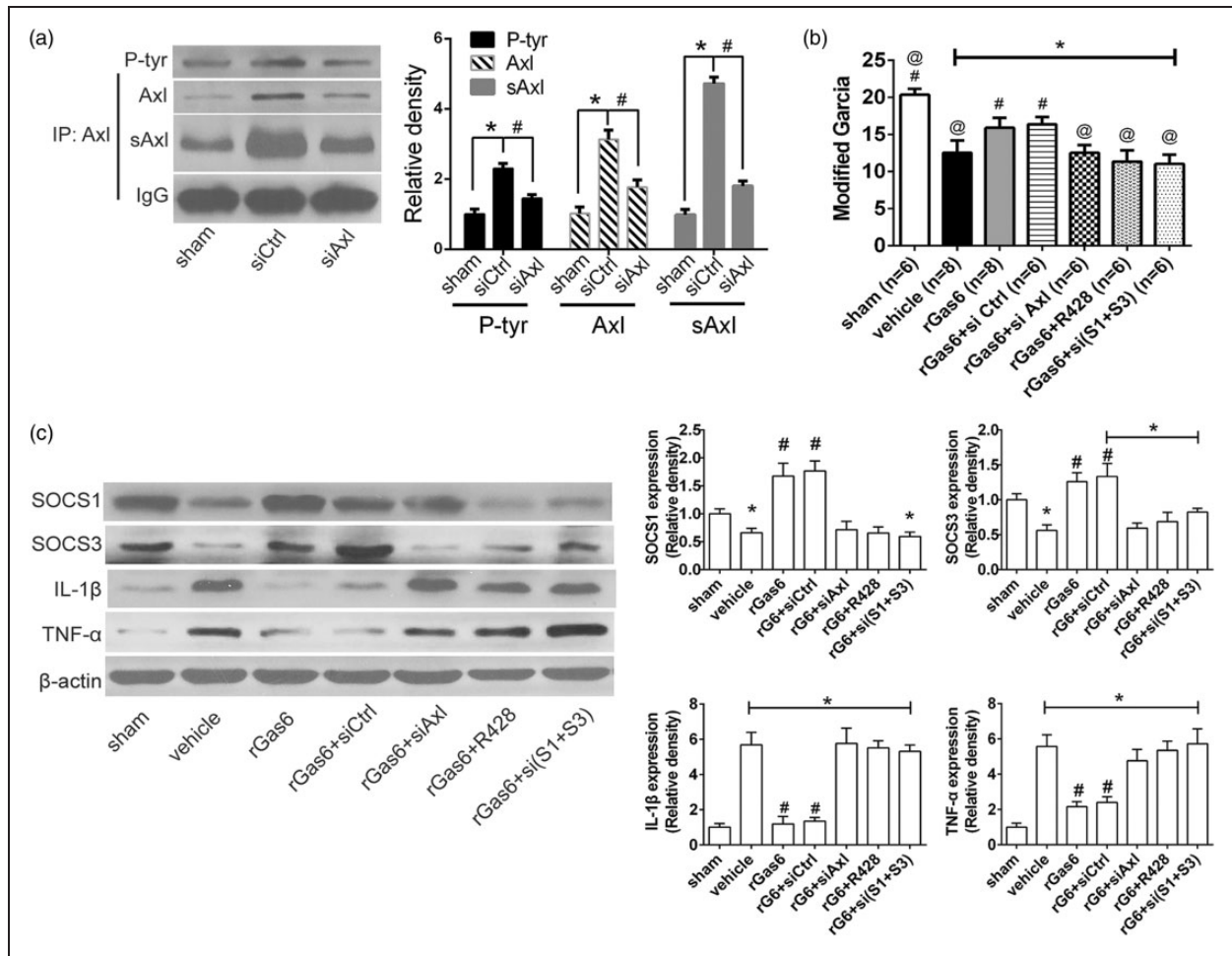


Figure 6. In vivo Axl knockdown reduced phosphorylated-Axl and soluble Axl, inhibited SOCSs signal and aggravated cytokine releasing. (a) Immunoprecipitating assay and quantification for Axl, phosphorylated Axl, and soluble Axl at 24 h following bICH in sham, ICH model with control or Axl siRNA. (b) Modified Garcia score evaluating neurobehavioral function in sham, vehicle, rGas6, rGas6+control siRNA, rGas6+si Axl, rGas6+R428, rGas6+si (SOCS1+SOCS3). (c) Western blot assays detecting expression of SOCS1, SOCS3, TNF- α and IL-1 β in sham, vehicle, rGas6, rGas6+control siRNA, rGas6+si Axl, rGas6+R428, rGas6+si (SOCS1+SOCS3). $n=6/8$ mice each group. si(S1+S3) represents si(SOCS1+SOCS3), rG6 represents recombinant Gas6. Error bars represented median \pm standard deviation. * $p < 0.05$ versus sham; # $p < 0.05$ versus ICH+control siRNA in (a), @ $p < 0.05$ versus rGas6 for (b); # $p < 0.05$ versus vehicle for (b) and (c).

indicated SOCSs proteins as key factors in controlling inflammatory response subsequent to ICH. Recently, factors other than Janus Kinases/the Signal Transducers and Activators of Transcription (JAK/STAT)^{35,36} were found that substantially regulate SOCSs, such as Axl⁷ and miR-155.³⁷ In our experiments, the upregulation of SOCSs expression was consistent with rGas6-induced Axl activation. In contrast, blockade of Axl signal with R428 and Axl-siRNA both reduced SOCSs expression. Together these results suggested that activated Axl signal may be a substantial inducer of SOCS1 and SOCS3 in ICH model.

Previous studies elucidated the neuroprotective role of Gas6 in the model of multiple sclerosis^{38,39} and EAE.¹¹ In these studies, Axl was involved to mediate

phagocytosis of apoptotic cells and neurogenesis which contributed to attenuating inflammation. But these indirect effects to inflammation were not referred to in the present study. Further study about other roles of Axl signal in ICH settings is needed. Another limitation in our study was that only male mice were utilized. Thus, we were unable to investigate into the difference between the two genders of Axl signaling, neither the gender effect in ICH. Therefore, we should be more cautious when interpreting these results.

A novel opinion in the present study is that, a potential narrow therapeutic time window exists for ICH treatment. We did not simply inhibit an inflammatory key factor as previous studies did, as more and more studies have revealed dual roles for certain

“inflammatory factors” we defined before. For example, thrombin was found pro-inflammatory, while essential to stop bleeding and brain recovery after ICH.^{40,41} Thus in this study, we chose to augment the impaired key factor to strengthen the immune restoration in early phase before the inflammatory cascades became overwhelmed.

In conclusion, our findings suggested that Axl signal may contribute to the immune restoration after ICH, and rGas6 administration can augment this neuroprotective effect. This signal was most likely mediated by intracellular phosphorylation and cleavage of ectodermal portion of Axl, and SOCSs upregulation was followed. Therefore, Axl signaling may be a potential target for ICH immune restoration.

Funding

The author(s) disclosed receipt of the following financial support for the research, authorship, and/or publication of this article: This work was supported by grants NS082184 from National Institute of Health to J.H. Zhang, and National Natural Science Foundation of China (NSFC) (81500991) to L.S. Tong.

Declaration of conflicting interests

The author(s) declared no potential conflicts of interest with respect to the research, authorship, and/or publication of this article.

Authors' contributions

JHZ, ML, JPT, LST, and AWS conceived and designed the study. LST, AWS, YBO, ZNG, and AM collected and analyzed the data. ZNG, AM, and BJD contributed in the data analysis and drafting the article. And all the authors (LST, AWS, YBO, ZNG, AM, BJD, JPT, ML, and JHZ) contributed towards the study design, drafting of the article.

Supplementary material

Supplementary material for this paper can be found at <http://jcbfm.sagepub.com/content/by/supplemental-data>

References

- Keep RF, Hua Y and Xi G. Intracerebral haemorrhage: mechanisms of injury and therapeutic targets. *Lancet Neurol* 2012; 11: 720–731.
- Zhou Y, Wang Y, Wang J, et al. Inflammation in intracerebral hemorrhage: from mechanisms to clinical translation. *Prog Neurobiol* 2014; 115: 25–44.
- Xi G, Strahle J, Hua Y, et al. Progress in translational research on intracerebral hemorrhage: Is there an end in sight? *Prog Neurobiol* 2014; 115: 45–63.
- Zhao H, Garton T, Keep RF, et al. Microglia/macrophage polarization after experimental intracerebral hemorrhage. *Transl Stroke Res* 2015; 6: 407–409.
- Schlunk F and Greenberg SM. The pathophysiology of intracerebral hemorrhage formation and expansion. *Transl Stroke Res* 2015; 6: 257–263.
- Rothlin CV, Carrera-Silva EA, Bosurgi L, et al. Tam receptor signaling in immune homeostasis. *Ann Rev Immunol* 2015; 33: 355–391.
- Lemke G and Rothlin CV. Immunobiology of the tam receptors. *Nat Rev Immunol* 2008; 8: 327–336.
- Zagorska A, Traves PG, Lew ED, et al. Diversification of tam receptor tyrosine kinase function. *Nat Immunol* 2014; 15: 920–928.
- Rothlin CV, Ghosh S, Zuniga EI, et al. Tam receptors are pleiotropic inhibitors of the innate immune response. *Cell* 2007; 131: 1124–1136.
- van den Brand BT, Abdollahi-Roodsaz S, Vermeij EA, et al. Therapeutic efficacy of tyro3, axl, and mer tyrosine kinase agonists in collagen-induced arthritis. *Arthritis Rheum* 2013; 65: 671–680.
- Gruber RC, Ray AK, Johndrow CT, et al. Targeted gas6 delivery to the cns protects axons from damage during experimental autoimmune encephalomyelitis. *J Neurosci* 2014; 34: 16320–16335.
- Rynkowski MA, Kim GH, Komotar RJ, et al. A mouse model of intracerebral hemorrhage using autologous blood infusion. *Nature Protocols* 2008; 3: 122–128.
- Ma Q, Chen S, Hu Q, et al. Nlrp3 inflammasome contributes to inflammation after intracerebral hemorrhage. *Ann Neurol* 2014; 75: 209–219.
- Topkoru BC, Altay O, Duris K, et al. Nasal administration of recombinant osteopontin attenuates early brain injury after subarachnoid hemorrhage. *Stroke* 2013; 44: 3189–3194.
- Garcia JH, Wagner S, Liu KF, et al. Neurological deficit and extent of neuronal necrosis attributable to middle cerebral artery occlusion in rats. Statistical validation. *Stroke* 1995; 26: 627–634. discussion 635.
- Hua Y, Schallert T, Keep RF, et al. Behavioral tests after intracerebral hemorrhage in the rat. *Stroke* 2002; 33: 2478–2484.
- Krafft PR, Caner B, Klebe D, et al. Pha-543613 preserves blood-brain barrier integrity after intracerebral hemorrhage in mice. *Stroke* 2013; 44: 1743–1747.
- Huang L, Sherchan P, Wang Y, et al. Phosphoinositide 3-kinase gamma contributes to neuroinflammation in a rat model of surgical brain injury. *J Neurosci* 2015; 35: 10390–10401.
- Zhang Y, Chen Y, Wu J, et al. Activation of dopamine d2 receptor suppresses neuroinflammation through alphab-crystalline by inhibition of nf-kappab nuclear translocation in experimental ich mice model. *Stroke* 2015; 46: 2637–2646.
- Xiong XY and Yang QW. Rethinking the roles of inflammation in the intracerebral hemorrhage. *Transl Stroke Res* 2015; 6: 339–341.
- Chen S, Yang Q, Chen G, et al. An update on inflammation in the acute phase of intracerebral hemorrhage. *Transl Stroke Res* 2015; 6: 4–8.
- Wang YC, Wang PF, Fang H, et al. Toll-like receptor 4 antagonist attenuates intracerebral hemorrhage-induced brain injury. *Stroke* 2013; 44: 2545–2552.

23. Fu Y, Hao J, Zhang N, et al. Fingolimod for the treatment of intracerebral hemorrhage: a 2-arm proof-of-concept study. *JAMA Neurol* 2014; 71: 1092–1101.
24. Selim M and Sheth KN. Perihematoma edema: a potential translational target in intracerebral hemorrhage? *Transl Stroke Res* 2015; 6: 104–106.
25. Rothlin CV and Lemke G. Tam receptor signaling and autoimmune disease. *Curr Opin Immunol* 2010; 22: 740–746.
26. Xu J, Ma F, Yan W, et al. Identification of the soluble form of tyrosine kinase receptor Axl as a potential biomarker for intracranial aneurysm rupture. *BMC Neurol* 2015; 15: 23.
27. Read SA, Tay ES, Shahidi M, et al. Hepatitis c virus driven axl expression suppresses the hepatic type i interferon response. *PLoS One* 2015; 10: e0136227.
28. Ekman C, Jonsen A, Sturfelt G, et al. Plasma concentrations of gas6 and saxl correlate with disease activity in systemic lupus erythematosus. *Rheumatology* 2011; 50: 1064–1069.
29. Giangola MD, Yang WL, Rajayer SR, et al. Growth arrest-specific protein 6 attenuates neutrophil migration and acute lung injury in sepsis. *Shock (Augusta, Ga.)* 2013; 40: 485–491.
30. Costa M, Bellosta P and Basilico C. Cleavage and release of a soluble form of the receptor tyrosine kinase ark in vitro and in vivo. *J Cell Physiol* 1996; 168: 737–744.
31. Scutera S, Fraone T, Musso T, et al. Survival and migration of human dendritic cells are regulated by an ifn-alpha-inducible axl/gas6 pathway. *J Immunol* 2009; 183: 3004–3013.
32. Verma A, Warner SL, Vankayalapati H, et al. Targeting axl and mer kinases in cancer. *Mol Cancer Ther* 2011; 10: 1763–1773.
33. Kimura A, Naka T, Muta T, et al. Suppressor of cytokine signaling-1 selectively inhibits lps-induced il-6 production by regulating jak-stat. *Proc Natl Acad Sci U S A* 2005; 102: 17089–17094.
34. Fenner JE, Starr R, Cornish AL, et al. Suppressor of cytokine signaling 1 regulates the immune response to infection by a unique inhibition of type i interferon activity. *Nat Immunol* 2006; 7: 33–39.
35. Yoshimura A, Naka T and Kubo M. Socs proteins, cytokine signalling and immune regulation. *Nat Rev Immunol* 2007; 7: 454–465.
36. Babon JJ and Nicola NA. The biology and mechanism of action of suppressor of cytokine signaling 3. *Growth Factors* 2012; 30: 207–219.
37. Cardoso AL, Guedes JR, Pereira de Almeida L, et al. Mir-155 modulates microglia-mediated immune response by down-regulating socs-1 and promoting cytokine and nitric oxide production. *Immunology* 2012; 135: 73–88.
38. Binder MD, Cate HS, Prieto AL, et al. Gas6 deficiency increases oligodendrocyte loss and microglial activation in response to cuprizone-induced demyelination. *J Neurosci* 2008; 28: 5195–5206.
39. Tshiperson V, Li X, Schwartz GJ, et al. Gas6 enhances repair following cuprizone-induced demyelination. *PLoS One* 2010; 5: e15748.
40. Hua Y, Keep RF, Gu Y, et al. Thrombin and brain recovery after intracerebral hemorrhage. *Stroke* 2009; 40(3 Suppl): S88–S89.
41. Coughlin SR. Thrombin signalling and protease-activated receptors. *Nature* 2000; 407: 258–264.